frontiers | Frontiers in Soil Science

TYPE Original Research
PUBLISHED 09 February 2026
DOI 10.3389/fsoil.2026.1724235

OPEN ACCESS

EDITED BY
Jose Navarro Pedreño,
Miguel Hernández University of Elche, Spain

REVIEWED BY
Jalal Kassout,
National Institute for Agricultural Research (Morocco), Morocco
Francesco De Mastro,
University of Bari Aldo Moro, Italy
Abhishek Nandal,
Maharshi Dayanand University, India

*CORRESPONDENCE
Russell Poma-Chamana
rpomac7@gmail.com

RECEIVED 13 October 2025
REVISED 20 January 2026
ACCEPTED 21 January 2026
PUBLISHED 09 February 2026

CITATION
Poma-Chamana R, Vilca-Gamarra C, Linares-Escapa S, Puma-Huacani K, Carrillo A, Villalta Soto MJC and Quispe K (2026) Soil quality in olive orchards of southern Peru using a weighted soil quality index (SQIw): constraints by salinity, organic matter and sustainable management approach. *Front. Soil Sci.* 6:1724235. doi: 10.3389/fsoil.2026.1724235

Soil quality in olive orchards of southern Peru using a weighted soil quality index (SQIw): constraints by salinity, organic matter and sustainable management approach

Russell Poma-Chamana[1]*, Cesar Vilca-Gamarra[1], Solmayra Linares-Escapa[1], Katherine Puma-Huacani[1], Alex Carrillo[1], Martín J. C. Villalta Soto[2] and Kenyi Quispe[3]

[1]Dirección de Servicios Estratégicos Agrarios, Estación Experimental Agraria Arequipa, Instituto Nacional de Innovación Agraria (INIA), Arequipa, Peru, [2]Agronomy Department, Universidad Nacional de San Agustín, Arequipa, Peru, [3]Dirección de Servicios Estratégicos Agrarios, Instituto Nacional de Innovación Agraria (INIA), Lima, Peru

Introduction: Soil salinization and alkalinization in the arid zones of southern Peru pose major challenges to agricultural sustainability, particularly in the olive orchards of Bella Unión, where irrigation relies on surface and groundwater of variable quality. This study aimed to assess soil quality and its spatial variability to support site-specific management in olive (*Olea europaea L* L.) orchards.
Methods: A total of 160 composite soil samples (0–30 cm) were collected from representative olive orchards and analyzed for pH, electrical conductivity (ECe), organic matter (OM), available phosphorus (Pav), available potassium (Kav), texture, and calcium carbonate equivalent (CCE). The Soil Quality Index (SQIw) was calculated and combined with multivariate and geostatistical analyses to identify key soil quality indicators and characterize their spatial variability.
Results: Soils showed high variability in salinity (ECe = 1.30–24.61 dS m^{-1}) and organic matter content (0.50–3.10%), while pH was relatively homogeneous (6.90–8.40). According to the SQIw, 1.26% of soils were classified as Very Poor, 44.96% as Poor, 51.49% as Acceptable, 2.28% as Good, and 0.01% as Optimal. Electrical conductivity was the main factor controlling the SQIw.
Discussion: These results indicate that salinity represents a major constraint for olive growth and productivity in the study area. Despite its lower weight in the SQIw, the generally low organic matter levels suggest limitations for soil fertility, water retention, and nutrient cycling, highlighting the need for organic amendments with low electrical conductivity. Nutrient management should also account for reduced nutrient availability under alkaline–saline conditions and the widespread organic matter deficiency. This study represents the first application of SQIw in Peruvian olive orchards and demonstrates its usefulness for delineating low-quality zones, guiding fertilization and soil recovery strategies, and promoting sustainable soil management in arid agroecosystems.

KEYWORDS

arid agroecosystems, geostatistics, olive, site-specific management, soil quality index

1 Introduction

Soils play a central role in sustaining agricultural productivity and ecosystem functioning (1). However, in arid and semiarid regions, soil quality is increasingly threatened by salinization and alkalinity, processes often intensified by irrigation practices and poor water quality (2–4). Currently, more than 1.3 billion hectares of land worldwide are affected by salt-related degradation, posing a major limitation to crop performance and long-term soil sustainability (4). Soil salinity therefore represents a significant barrier to agricultural resilience in water-limited regions.

Olive (*Olea europaea L.*) is a key perennial species in arid and Mediterranean-type ecosystems due to its ecological plasticity and socioeconomic relevance, particularly for smallholder farmers (5, 6). Its tolerance to salinity is supported by mechanisms such as selective ionic exclusion, salt sequestration in roots, maintenance of optimal K^+/Na^+ ratios, osmotic adjustment, and activation of antioxidant systems (7). However, this tolerance has limits: yield losses of ~10% occur when soil electrical conductivity (ECe) exceeds 4–6 dS m^{-1} (8). Higher salinity levels reduce vegetative growth, total biomass (up to 87%), oil content, and fruit weight, while increasing fruit moisture and altering fatty acid composition (9–11). Field reports from Israel and Tunisia demonstrate that prolonged irrigation with brackish water can progressively reduce olive productivity (12, 13), suggesting strong environmental context-dependency.

Given these constraints, soil-based diagnostics are essential in arid agricultural systems, where soil properties such as salinity, pH, and fertility show pronounced spatial variability influenced by irrigation type, water quality, and heterogeneous management (14). The Soil Quality Index (SQI) framework provides an integrative approach to evaluate degradation processes and synthesize multiple indicators into a single metric to support agricultural decision-making (15, 16). Weighted-SQI approaches have demonstrated strong suitability in arid landscapes for identifying fertility gradients, characterizing salinity impacts, and delineating management zones using statistical and geospatial techniques (17–19). Applications in Kenya and Tunisia demonstrate the sensitivity of weighted SQIs to soil sustainability and salinization processes (20, 21), and research in Iran underscores the importance of context-specific indicator selection and calculation method (22). Methodological advances, including geostatistics, computational intelligence, and sampling optimization, continue to strengthen the framework's relevance in heterogeneous arid systems.

Despite these advances, SQI applications remain scarce in olive-based systems in Peru and comparable coastal desert agroecosystems in South America. Bella Unión, located on the southern Peruvian coast, is emerging as an increasingly important olive-producing area; however, the system faces constraints linked to historical salinity, variable irrigation water quality, and limited soil monitoring (23, 24). Although no official yield statistics are available, informal reports from growers and local agronomic advisors suggest possible stagnation or decline in productivity in some orchards, particularly where soil salinity may be increasing. This problem is worsened by the very low use of soil testing in the country. Only 1.3% of producers carry out soil analyses with technical assistance, which greatly limits informed management decisions (25).

Given this context, a spatially explicit assessment of soil quality is necessary to support sustainable intensification and guide precision management. Therefore, the objective of this study was to develop a Soil Quality Index tailored to olive orchards in Bella Unión, Peru, and to generate spatial soil quality maps to identify management zones and inform agronomic recommendations under arid irrigated conditions.

Based on prior literature, we hypothesized that soil quality in olive orchards of Bella Unión exhibits significant spatial variability and that the Soil Quality Index would differentiate distinct soil quality classes relevant to decision-making under arid irrigated conditions. Additionally, we expected that salinity-related indicators would be the primary constraints affecting soil quality in the study area.

2 Materials and methods

2.1 Study area

The present study was carried out in the Bella Unión irrigation scheme, located in the Bella Unión District, Caravelí Province, Department of Arequipa (Figure 1). This site is situated between latitudes 15°27′15″S and 15°30′15″S and longitudes 74°37′30″W and 74°45′0″W, covering an agricultural area of 3872.02 ha (26). The average altitude is 225 m above sea level, with elevations ranging from 192 to 232 m. The geomorphology of the area is composed of alluvial terraces (95%), with smaller percentages of alluvial slopes (4%) and sand layers (1%) (27). This area is characterized by arid climate conditions, scarce precipitation (nearly 5 mm annually) (28), and a dependence on irrigation for agricultural activity (29). The predominant cultivation in the area is the Sevillana variety of olive, along with temporary crops on a smaller scale.

2.2 Sampling and soil analysis

A total of 160 composite soil samples were collected between July and August 2024 using a random sampling scheme in commercial orchards of approximately 1 ha, spatially distributed to capture the heterogeneity of the study area (Figure 1). Orchard selection was conditioned by the voluntary willingness of farmers to participate and grant access to their fields. Within each selected orchard, a systematic zig-zag sampling pattern between trees was followed to capture within-field spatial variability (30).

The number of trees sampled per orchard was adjusted according to planting density: 8 trees in orchards with spacings ≥ 10 × 10 m (≤ 100 trees ha^{-1}) and 10 trees in higher-density orchards (6 × 6 m, 6 × 7 m, 7 × 7 m; > 200 trees ha^{-1}). For each selected tree, two subsamples were collected at a depth of 0–30 cm using a shovel, located at two opposite cardinal points (180°) within the irrigation

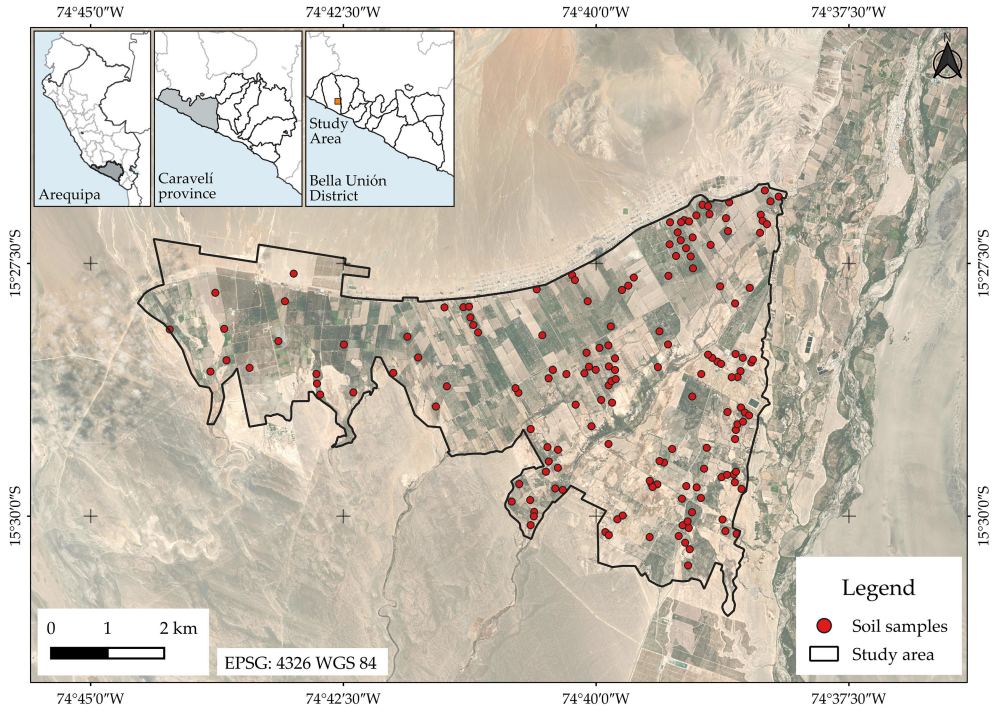

FIGURE 1
Location of soil sampling sites.

basin, in order to capture spatial variability, partially following the approach described by (31), who collected four subsamples per tree, one at each cardinal point. Consequently, each composite sample (0.8–1.0 kg) integrated between 16 and 20 individual subsamples (8–10 trees × 2 subsamples per tree), exceeding in many sampling points the recommended range of 4–16 subsamples (32), and following a composite sampling approach similar to that described by (33), who applied soil sampling around tree-based microsites for soil quality assessment. All subsamples from the same orchard were thoroughly homogenized in a clean, non-galvanized container to form the composite sample. Finally, the samples were sealed in double plastic bags, labeled with unique identifiers, and georeferenced using a handheld GPS unit (± 3 m accuracy).

Samples were analyzed at the Soil, Water and Foliar Laboratory Network of the National Institute of Agrarian Innovation (LABSAF-INIA), Peru, as part of a national soil fertility monitoring program. Analytical protocols are standardized for high sample throughput, focusing on essential fertility indicators rather than exhaustive geochemical speciation. Prior to physicochemical analysis, samples were air-dried (< 40°C), and sieved to obtain a < 2 mm fraction, according to the procedure of the International Organization for Standardization (34). The variables analyzed included the following parameters and reference methodologies: sand, silt and clay content by the Bouyoucos hydrometer method (35); pH measured in a 1:1 soil-water suspension according to the United States Environmental Protection Agency method (36); electrical conductivity in a 1:5 soil-water extract (EC1:5) (37); organic matter (OM) by the Walkley–Black oxidation method; available phosphorus (Pav) by the Olsen method; available potassium (Kav) by 1N ammonium acetate extraction; and calcium carbonate (CCE) via acid neutralization (35). Although ECe is the standard for salinity assessment, EC1:5 was measured given its suitability for large-scale laboratory operations; the conversion procedure to ECe values is addressed in the following section.

2.3 Estimation of saturated paste electrical conductivity

To convert the measured EC1:5 into the standard ECe metric while minimizing errors associated with soil texture variability, the model proposed by (38) was applied. Unlike fixed conversion factors, this approach explicitly incorporates sand and clay contents into the conversion factor calculation, making it appropriate for texturally heterogeneous areas. This model was developed using 148 soil samples from coastal areas of Greece under arid and semiarid conditions, with sand contents ranging from 3.6% to 84.6% and clay contents from 7.4% to 48.5%, an environmental setting comparable to the Bella Unión district. The estimation was performed according to Equation 1:

$$EC_e = \left(1.054 + \frac{283.4}{49.699 + 0.524 \cdot \text{Clay}\,\% - 0.339 \cdot \text{Sand}\,\%}\right) \cdot EC_{1:5} \quad (1)$$

To assess the uncertainty associated with the indirect estimation of ECe, a sensitivity analysis was conducted following the error propagation framework for pedotransfer functions described by (39). This analysis evaluated the propagation of textural variability

into ECe estimates by perturbing sand and clay contents by ±1 standard deviation of the observed values. The total uncertainty was calculated by combining this texture-related error with the inherent model error (RMSE = 1.39 dS m^{-1}) reported by (38), using standard error propagation methods. As a final step, we verified whether the estimated uncertainty altered the salinity classification, thereby securing the practical validity of the delineated zones.

2.4 Weighted soil quality index development

The development of the SQIw followed a three-stage methodological framework: (1) screening soil indicators to establish a Minimum Data Set (MDS); (2) transforming indicators into dimensionless scores; and (3) integrating scores into a weighted index.

2.4.1 Minimum data set selection

To minimize data redundancy and identify the most representative indicators, a screening process was applied to the Total Data Set (TDS). Spearman's rank correlation coefficients were computed to assess the degree of association among all variable pairs and detect potential multicollinearity. Significant correlations ($p < 0.01$) were visualized using correlation matrix heatmaps to identify redundant variable groups. Indicator pairs exhibiting strong redundancy were defined as those with absolute correlation coefficients greater than 0.70 ($|\rho| > 0.70$). For each group of redundant variables, a single representative was selected based on its agronomic significance for soil quality assessment in arid agroecosystems. Redundant variables were subsequently excluded.

The retained variables were standardized to zero mean and unit variance. Principal Component Analysis (PCA) was performed to identify dominant patterns of multivariate variation and derive quantitative weights for each indicator. Principal Components (PCs) with eigenvalues ≥ 1 were retained according to the Kaiser criterion, while aiming to explain at least 60% of cumulative variance. Factor loadings were calculated for each variable within each retained PC to quantify variable contributions to component variance.

Variables were evaluated against two explicit selection criteria to determine final inclusion in the MDS. Candidates had to both demonstrate factor loading magnitude greater than 0.60 within retained PCs (confirming measurable contribution to the multivariate structure) and represent either critical soil functions (e.g., nutrient cycling, moisture retention) or physical/chemical constraints in arid environments. Only variables satisfying both criteria were retained in the final MDS.

2.4.2 Indicator transformation and scoring

Selected MDS indicators were transformed into dimensionless scores ranging from 0.1 to 1.0 to compare soil variables measured in different units. This scaling range allows limiting factors to significantly penalize the final score without assigning a zero value, thereby acknowledging that even degraded soils retain a baseline functional capacity.

A hybrid approach was adopted to define critical thresholds (x_1 and x_2), integrating agronomic requirements for olive cultivation with the specific statistical distribution of data observed in the study area (Table 1). Following (40) for arid agroecosystems, the lower threshold for Organic Matter (OM) was anchored to the minimum value in the dataset. This normalization according to local soil conditions avoids artificially penalizing arid soils against unattainable temperate standards. To accurately reflect the water retention capacity required for optimal soil functioning, the upper threshold (x_2) was maintained at the physiological optimum described by (41). Similarly, the upper thresholds for macronutrients (Pav, Kav) were set to the maximum observed values in the dataset. This relative scoring approach enables a clearer distinction between the "best" and "worst" soils within the valley, preventing the score saturation that typically occurs when local nutrient concentrations exceed standard crop optima. Similarly, the upper threshold for pH was extended to 8.5 to capture the full alkaline gradient without premature penalization. Regarding Salinity (ECe), the lower threshold (x_1 = 2.0 dS m^{-1}) was aligned with the USDA standard for non-saline soils (42), ensuring optimal scoring for conditions free of osmotic stress. The upper threshold (x_2) was set at 12.0 dS m^{-1}, a critical level where yield losses become severe due to osmotic inhibition (8). For Sand content, thresholds were established based on documented relationships between particle size and critical soil functions. The upper threshold (x_2 = 52%) represents the transition beyond which soils exhibit insufficient water-holding capacity (< 0.10 cm^3 cm^{-1}) and reduced nutrient retention, characteristic of "primarily sandy" textures (43, 44). Conversely, the lower threshold (x_1 = 23%) marks the boundary with silt-dominated textures; values below this limit

TABLE 1 Scoring functions and threshold values for soil quality indicators.

Indicator	Unit	Function	Lower threshold (x_1)	Upper threshold (x_2)
OM	%	MB	0.5	5.0
Pav	mg kg^{-1}	MB	5	74
Kav	mg kg^{-1}	MB	40	488
pH	–	LB	7.0	8.5
ECe	dS m^{-1}	LB	2.0	12.0
Sand	%	LB	23	52

LB, the lower, the better; MB, the more, the better. OM, Organic Matter; Pav, Available Phosphorus; Kav, Available Potassium; ECe, Electrical Conductivity of saturation extract.

are scored optimally, reflecting that water retention capacity outweighs drainage concerns in this rainfed semi-arid context.

After establishing thresholds, indicators were standardized using linear scoring methods to assign a score to each variable, following the principles described by (45). The indicators were transformed according to their functional influence on soil quality, where the "More is better" (MB) function (Equation 2) was applied to OM, Pav, and Kav as their availability correlates positively with fertility. Conversely, the "Less is better" (LB) function (Equation 3) was adopted for Salinity (ECe), Sand content, and pH, with pH selected specifically because observed values consistently exceeded the neutral threshold (> 7.0).

$$M(x) = \begin{cases} 0.1\ , & x \le x_1 \\ 0.1 + 0.9\left(\frac{x-x_1}{x_2-x_1}\right)\ , & x_1 < x < x_2 \\ 1\ , & x \ge x_2 \end{cases} \quad (2)$$

$$L(x) = \begin{cases} 1\ , & x \le x_1 \\ 1 - 0.9\left(\frac{x-x_1}{x_2-x_1}\right), & x_1 < x < x_2 \\ 0.1\ , & x \ge x_2 \end{cases} \quad (3)$$

Where x is the measured value, and x_1 and x_2 denote the lower and upper threshold values, respectively.

2.4.3 Weight assignment and SQIw calculation

Weights for each MDS indicator were derived quantitatively from the PCA results to minimize subjective bias. The weight (Wi) for each indicator was calculated as the proportion of variance it explained relative to the cumulative variance of all retained PCs. The final Weighted Soil Quality Index (SQIw) was computed using the weighted additive approach (Equation 4):

$$SQI_w = \sum_{i=1}^{n} W_i N_i \quad (4)$$

where n is the total number of variables, W_i is the assigned weight, and N_i is the normalized indicator score. The resulting index was classified into five quality grades using equal intervals of 0.2, following the classification scheme used for agricultural soil fertility mapping (46). SQIw values were classified as follows: < 0.20 as "Very Poor"; 0.20–0.40 as "Poor"; 0.40–0.60 as "Acceptable"; 0.60–0.80 as "Good"; and ≥ 0.80 as "Optimal".

2.5 Spatial data analysis

2.5.1 Descriptive statistics

Descriptive statistics were calculated for all variables, including mean, minimum and maximum values, standard deviation (SD), coefficient of variation (CV), skewness, median with 25th–75th percentiles, and p-values from the Kolmogorov-Smirnov test of normality.

2.5.2 Exploratory spatial data analysis

Prior to spatial interpolation, an Exploratory Spatial Data Analysis (ESDA) was conducted to characterize the spatial structure of soil properties and guide the selection of the most appropriate interpolation method.

First, a spatial structure assessment was performed. Global spatial autocorrelation was evaluated for the SQIw and all selected soil indicators using Moran's I index (47) (Equation 5), which quantifies the degree to which similar values cluster spatially. An inverse distance spatial weight matrix based on the eight nearest neighbors (k = 8) was employed. Statistical significance was evaluated at $\alpha = 0.05$.

$$Moran's\ I = \frac{n}{\sum_{i=1}^{n}\sum_{j=1}^{n} w_{ij}} \cdot \frac{\sum_{i=1}^{n}\sum_{j=1}^{n} w_{ij}(y_i - \bar{y})(y_j - \bar{y})}{\sum_{i=1}^{n}(y_i - \bar{y})^2} \quad (5)$$

where n is the number of observations, w_{ij} is the spatial weight representing the degree of connection between neighboring samples i and j, y_i is the sampled value at location i, and $\bar{y}$ is the arithmetic mean of all sampled values. Moran's I values range from -1 to +1, where positive values indicate spatial clustering of similar values, values near zero suggest random spatial distribution, and negative values indicate spatial dispersion.

Empirical semivariograms were computed to examine the spatial dependence structure and estimate geostatistical parameters. Theoretical models (Gaussian, Spherical, and Exponential) were fitted to the empirical semivariograms, and the best fitting model for each variable was selected based on the lowest sum of squared errors. The following parameters were extracted: nugget effect (C_0), representing variance at zero distance; partial sill (C), representing spatially structured variance; total sill ($C_0 + C$); and range (a), the distance beyond which spatial correlation effectively disappears.

The nugget-to-sill ratio $[C_0/(C_0 + C)]$ was calculated to quantify the proportion of spatially structured variance relative to random noise or micro-scale variability, following the classification proposed by (48): strong spatial dependence (< 0.25), moderate (0.25–0.75), and weak (> 0.75).

To objectively evaluate interpolation approaches, the predictive performance of Inverse Distance Weighting (IDW) and Ordinary Kriging (OK) was compared using 10-fold-cross-validation. The dataset was randomly divided into 10 subsets, and each subset was iteratively used for validation while the remaining nine subsets were used for model fitting. Predictive accuracy was evaluated using four statistical metrics: Root Mean Square Error (RMSE) (Equation 6), Mean Absolute Error (MAE) (Equation 7), coefficient of determination (R^2) (Equation 8), and mean error (ME) (Equation 9). Lower RMSE and MAE values, higher R^2 values, and ME values close to zero indicate better predictive performance.

$$RMSE = \sqrt{\frac{1}{n}\sum_{i=1}^{n}(y_i - \hat{y}_i)^2} \quad (6)$$

$$MAE = \frac{1}{n}\sum_{i=1}^{n}|y_i - \hat{y}_i| \quad (7)$$

10.3389/fsoil.2026.1724235

$$R^2 = 1 - \frac{\sum_{I=1}^{n}(y_i - \hat{y}_i)^2}{\sum_{I=1}^{n}(y_i - \bar{y})^2} \quad (8)$$

$$ME = \frac{1}{n}\sum_{i=1}^{n}(y_i - \hat{y}_i) \quad (9)$$

were n is the number of observations, y_i is the observed (measured) value at location i, $\hat{y}_i$ is the predicted value at location i obtained through cross-validation, and $\bar{y}$ is the mean of all observed values.

2.5.3 Spatial interpolation

Inverse Distance Weighting (IDW) is a deterministic interpolation technique that estimates values at unsampled locations by calculating a weighted average of neighboring observations. The method assigns greater weights to data points located closer to the interpolation point, thereby lowering the influence of more distant points, with this effect controlled by a power parameter (49). The IDW interpolation was performed according to Equation 10:

$$\hat{y}_p = \frac{\sum_{i=1}^{n} \frac{y_i}{d_i^r}}{\sum_{i=1}^{n} \frac{1}{d_i^r}} \quad (10)$$

where $\hat{y}_p$ is the predicted value at the unsampled point p; y_i is the observed value at sampled point i; d_i is the distance between points p and i; and r is the power parameter, set to 2; and n is the number of neighboring points used for interpolation, limited to a maximum of 12.

2.6 Estimation of site-specific managements requirements

To formulate agronomic management recommendations based on the previously analyzed soil properties, two key calculations were performed. First, the amount of organic amendment needed to increase soil carbon to a target level was estimated. Second, the specific fertilization requirement for olive cultivation was determined. Detailed equations, coefficients, and numerical assumptions used in these calculations are provided in the Supplementary Material (Supplementary Method S1).

2.7 Statistical analysis

Data processing and statistical analyses were performed using R software v.4.5.2 (50). Descriptive statistics and normality tests (Kolmogorov-Smirnov) were calculated using the base R environment. Multivariate analysis, specifically the Principal Component Analysis (PCA), was conducted using *FactoMineR* package (51). For the geostatistical analysis, spatial structure assessment (Moran's I) and interpolation (IDW) were carried out using the *gstat* (52) and *sp* (53) packages. Correlation matrices were generated with *psych* (54) and *corrplot* (55).

3 Results

3.1 Estimation of soil salinity and descriptive statistics

Given the constraints of 1:5 extracts, ECe values were derived using the textured-based conversion model of (38). A sensitivity analysis confirmed the model's reliability for the study area, as the textural range of the samples (Sand: 15.0–87.0%; Clay: 4.5–30.0%) fell within the model's calibration domain. Due to the coarser texture of Bella Unión soils (mean sand 47.6%), the calculated conversion factor (CF) was higher than standard values, ranging from 6.29 to 12.51 (Mean = 8.56 ± 1.12).

The uncertainty analysis, which accounted for textural variability and model error (RMSE), yielded a mean total uncertainty of ± 2.09 dS m^{-1} (Figure 2). Although this uncertainty implies that 65.0% of samples linear classification thresholds, the overall salinity diagnosis remains robust: even when accounting for maximum uncertainty, 74.4% of the samples are consistently classified as moderately saline or higher (ECe ≥ 4 dS m^{-1}). This confirms that salinity is a structural characteristic of the valley and not an artifact of estimation errors.

Descriptive statistics revealed a marked spatial heterogeneity across the study zone, with coefficients of variation (CV) exceeding 30% for most edaphic parameters (Table 2). Salinity (ECe) emerged as the most variable property, exhibiting a broad range that quantitatively reflects the coexistence of non-saline areas with extreme salinity hotspots within the same irrigation scheme. In contrast, pH was remarkably homogeneous, indicating a generalized slightly alkaline condition. Regarding fertility, Organic Matter (OM) levels were critically low (< 1%) yet highly variable. Conversely, available phosphorus (Pav) and potassium (Kav) displayed elevated mean concentrations relative to critical deficiency thresholds. Normality tests (K-S) confirmed that the pH, ECe, OM, and Clay content indicators followed non-normal distributions ($p < 0.05$).

3.2 Multivariate analysis and minimum data set selection

Spearman's correlation analysis (Figure 3) revealed strong multicollinearity among particle size fractions, particularly between Sand and Silt ($\rho = -0.93$, $p < 0.001$), confirming their compositional redundancy. Consequently, Sand content was retained as the sole physical proxy for the multivariate analysis. Regarding chemical interactions, significant inverse associations emerged between Sand and fertility indicators, specifically with Kav ($\rho = -0.63$) and OM ($\rho = -0.46$). Interestingly, correlations within the nutrient group (OM, Pav, Kav) remained ($\rho < 0.50$), suggesting that each variable contributes unique agronomic information. Although Calcium Carbonate Equivalent (CCE) showed some association with texture, it was excluded from the final MDS to prioritize pH and Salinity (ECe) as the primary

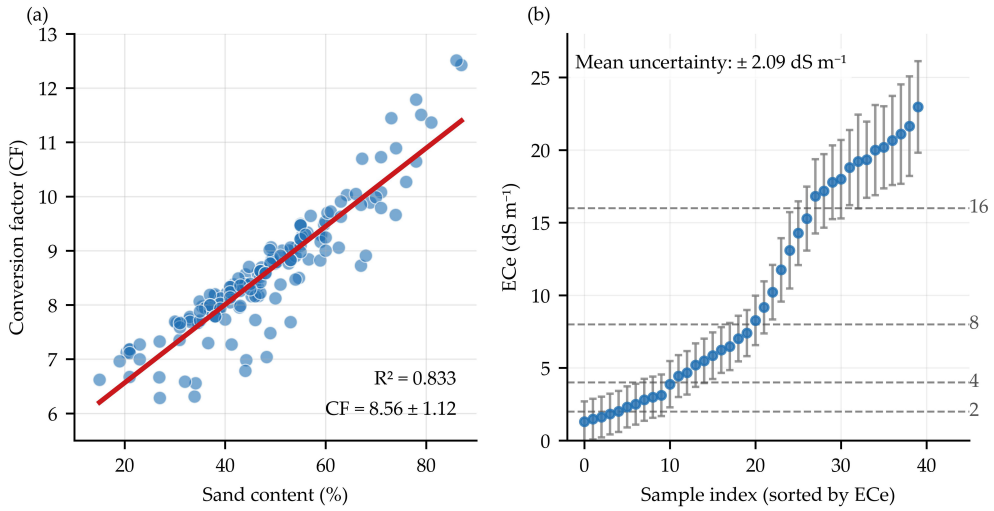

FIGURE 2
Sensitivity analysis of ECe estimation using the (38) texture-based conversion model. **(a)** Relationship between conversion factor (CF) and sand content, showing a strong positive correlation (R^2 = 0.833) that results in higher CF values for coarse-textured soils. **(b)** Estimated ECe values (n = 160) sorted in ascending order, with uncertainty bounds (mean ± 2.09 dS m^{-1}); dashed horizontal lines indicate salinity classification thresholds at 2, 4, 8, and 16 dS m^{-1}.

chemical constraints, which behaved as independent dimensions (ρ < 0.20 with most variables).

The Principal Component Analysis (PCA) performed on the selected MDS (Sand, pH, ECe, OM, Pav, Kav) extracted three components that cumulatively explain 76.52% of the total variance (Table 3). It is worth noting that the third component (PC3) was retained despite having an eigenvalue slightly below 1.0 (0.93), as it accounted for a substantial 15.5% of the variance, and captured the salinity constraint not represented in the first two components.

PC1 explained the largest proportion of variance (44.3%) and represented the fertility-texture complex. This component displayed high factor loadings for Sand (−0.81) versus Kav (0.80), OM (0.73) and Pav (0.72). The strong inverse relationship statistically highlights the pronounced contrast between sand content and fertility levels in the studied soils. PC2 (16.7% variance) was distinctly defined by pH (loading = 0.78), isolating alkalinity as an independent chemical dimension. Finally, PC3 (15.5%) was driven almost exclusively by Salinity (ECe) with a high positive loading (0.82), identifying it as a unique stressor distinct from general fertility patterns.

3.3 Soil quality index assessment

Based on the PCA weights, the specific Weighted Additive Index (SQIw) was established for the Bella Unión valley as presented in Equation 11. The structure of this equation reveals that Salinity (ECe) and Alkalinity (pH) exert a dominant influence on the model. Collectively, they represent 41.6% of the total index

TABLE 2 Descriptive statistics and normality test results of variables in the study area (n = 160).

Variable (Unit)	Mean ± SD	Median (Q_1 – Q_3)	Range (Min – Max)	CV (%)	Skewness	K-S test (*p*-value)
pH (1:1)	7.62 ± 0.22	7.60 (7.50 – 7.70)	6.90 – 8.40	3	0.32	0.004
ECe (ds m^{-1})	10.59 ± 7.35	8.23 (3.81 – 17.97)	1.30 – 24.61	69	0.29	< 0.001
OM (%)	0.95 ± 0.53	0.80 (0.50 – 1.30)	0.50 – 3.10	56	1.27	< 0.001
Pav (mg kg^{-1})	43.29 ± 9.98	41.2 (37.3 – 50.0)	6.9 – 74.0	23	-0.01	0.103
Kav (mg kg^{-1})	260.23 ± 88.92	255.3 (192.1 – 320.5)	105.2 – 488.2	34	0.45	0.489
Sand (%)	47.63 ± 14.23	46.6 (38.0 – 55.0)	15.0 – 87.0	30	0.35	0.582
Clay (%)	9.58 ± 4.80	8.0 (7.0 – 10.6)	4.5 – 30.0	50	2.22	< 0.001
Silt (%)	42.81 ± 14.81	44.3 (32.8 – 52.3)	4.0 – 73.0	35	-0.36	0.316
CCE (%)	3.08 ± 0.94	3.12 (2.57 – 3.70)	0.65 – 5.90	31	-0.23	0.752

SD, Standard Deviation; Q1, 25th percentile; Q3, 75th percentile; CV, Coefficient of Variation; K-S, Kolmogorov-Smirnov test; ECe, Electrical conductivity of the saturation extract; OM, Organic Matter; Pav, Available Phosphorus; Kav, Available Potassium; CCE, Calcium Carbonate Equivalent.

10.3389/fsoil.2026.1724235

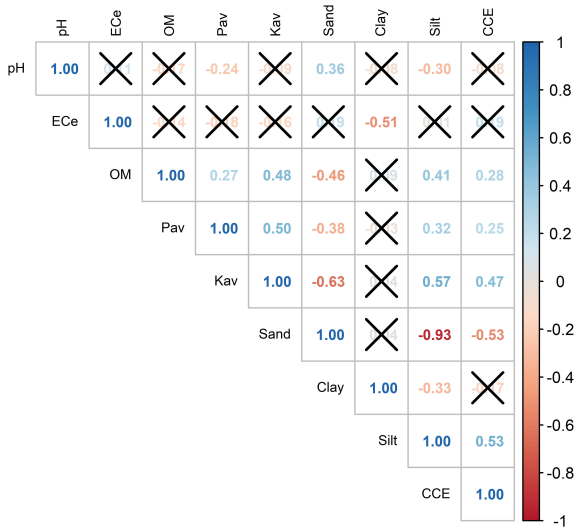

FIGURE 3
Spearman's correlation matrix of the Total Data Set (TDS) components for soil quality index assessment. Positive correlations are shown in blue, negative correlations in red, and X symbols represent non-significant associations. All displayed values are statistically significant at $p < 0.01$ level.

weight, confirming that these factors are the primary drivers of soil quality in the study area.

$$SQIw = 0.212 \cdot S_{ECe} + 0.204 \cdot S_{pH} + 0.177 \cdot S_{Kav} + 0.160 \cdot S_{Sand} + 0.123 \cdot S_{OM} + 0.123 \cdot S_{Pav} \quad (11)$$

Where S_i represents the normalized score (0.1-1) of each indicator.

Regarding the index performance, the sensitivity analysis of the baseline model initially detected a significant inverse correlation with salinity ($\rho = -0.73$, $p < 0.001$). While this coefficient suggested a general capacity to detect degradation, this data dispersion evidenced a masking effect in highly saline samples, where high nutrient levels (Pav and Kav) numerically compensated for the saline stress. The implementation of the Limiting Factor Correction, which restricts samples exceeding 8 dS m^{-1} to the "Poor" category, significantly enhanced the index's precision. This adjustment increased the correlation with salinity to $\rho = -0.86$ and resulted in the reclassification of 90% of the saline sites into categories that more accurately reflect their productive limitations.

Following this correction, the final assessment indicates that 15.6% of the soils correspond to the "Very Poor" category, 38.1% to "Poor", and 26.9% to "Acceptable". Only 18.8% of the area achieved the "Good" status, with a marginal 0.6% considered "Optimal". The observation that over 53% of the samples fall into the degraded strata quantitatively aligns with the high salinity observed (10.59 dS m^{-1}) across the irrigation scheme.

TABLE 3 PCA output including eigenvalues, percentage of variance explained, and factor loadings of component matrix variables.

PCs	PC1	PC2	PC3	PC4	PC5
Eigenvalue	**2.660**	**1.002**	**0.930**	0.634	0.504
Variance (%)	44.325	16.703	15.494	10.563	8.408
Cumulative Variance (%)	44.325	61.028	76.522	87.085	95.493
Factor loadings for each variable					
pH	-0.453	**0.784**	0.346	-0.087	-0.129
ECe (dS m^{-1})	-0.335	-0.436	**0.820**	0.123	0.094
OM (%)	**0.727**	0.099	0.167	-0.498	0.429
Pav (mg kg^{-1})	**0.720**	0.214	0.007	0.589	0.264
Kav (mg kg^{-1})	**0.799**	0.258	0.325	0.047	-0.257
Sand (%)	**-0.810**	0.275	-0.055	0.119	0.399

Principal Components (PCs) with eigenvalues > 0.9 were retained. Bold values indicate the dominant indicators within each PC based on absolute factor loadings > 0.60.

3.4 Geostatistical analysis and spatial distribution

Exploratory spatial data analysis (ESDA) revealed distinct spatial patterns among the soil indicators. Global Moran's I values were compared against the expected value under spatial randomness (−0.006), with statistical significance evaluated at $\alpha = 0.05$ (Table 4). Six out of seven variables exhibited statistically significant spatial autocorrelation, ranging from weak to moderate dependence. Sand content displayed the strongest spatial structure ($I = 0.254$), indicating high spatial continuity across the sampling area. Salinity (ECe) and phosphorus (Pav) also showed moderate autocorrelation ($I \approx 0.19$), while the weighted Soil Quality Index (SQIw), organic matter (OM), and available potassium (Kav) exhibited weaker but statistically significant spatial dependence ($I < 0.10$). In contrast, pH showed no significant spatial autocorrelation ($I = 0.038$, $p = 0.110$), presenting a random spatial pattern consistent with its low variability (CV = 3%) across the irrigation scheme.

TABLE 4 Global Moran's I index for spatial autocorrelation of soil properties and soil quality index.

Variable	Moran's I	Expected	Variance	Z-score	P-value
pH	0.038	-0.006	0.001	1.228	0.110
ECe (dS m^{-1})	0.196	-0.006	0.001	5.575	< 0.001
OM (%)	0.076	-0.006	0.001	2.288	0.011
Pav (mg kg^{-1})	0.187	-0.006	0.001	5.362	< 0.001
Kav (mg kg^{-1})	0.067	-0.006	0.001	2.027	0.021
Sand (%)	0.254	-0.006	0.001	7.211	< 0.001
SQIw	0.096	-0.006	0.001	2.830	0.002

Semivariogram analysis indicated moderate to strong spatial dependence for all variables (Supplementary Table S3, Supplementary Figure S1). Nugget-to-sill ratios ranged from 0.00 (pH) to 0.68 (OM), with only pH and sand content exhibiting strong spatial structure (ratio < 0.25). The majority of variables showed moderate dependence with ratios exceeding 0.50, indicating substantial short-range variability. Effective ranges varied from 144 m (pH) to 864 m (OM), with most variables showing partial correlation within 400 to 850 m, indicating different scales of spatial continuity. Model fits included Spherical (ECe, OM, Kav, SQIw), Gaussian (pH, Pav), and Exponential (Sand) forms.

Ten-fold cross-validation indicated comparable performance between IDW and Ordinary Kriging (Supplementary Table S4). Although OK yielded marginally lower RMSE values for six of the seven variables, the relative improvement was minimal (ranging from 2% to 10%), with absolute differences remaining below 7% across all soil properties. Overall, both interpolation methods demonstrated low predictive capacity (R^2 < 0.30) and negligible systematic bias ($|ME|$ < 4), indicating that neither the deterministic nor the geostatistical approach could adequately capture the short-range variability observed in the dataset. Consequently, given that Ordinary Kriging offered only a negligible improvement in RMSE while requiring complex stationarity assumptions not fully supported by the weak spatial structure, Inverse Distance Weighting (IDW) was selected as the final interpolation method. IDW was preferred for its ability to preserve local extreme values (hotspots) of salinity and organic matter without the smoothing effect typical of Kriging, providing a more conservative representation for management decisions in this highly heterogeneous system.

Spatial interpolation (Figure 4) reveals distinct soil patterns. Salinity (ECe) peaks (16.0–25.0 dS m^{-1}) in the southern and central-eastern sectors, while strongly salinity (8.0–16.0 dS m^{-1}) extends across much of the east. These areas generally correspond to pH values of 7.3–7.7. Sand content is highest in the central-northern sector (50.0–70.0%), whereas the western zone shows finer textures (20.0–50.0%). Organic matter (OM) is critically low (< 1.0%) across almost the entire study area, with only small localized patches exceeding 1.5%. Nutrient availability shows contrasting patterns: Available phosphorus (Pav) reaches its highest levels (> 45.0 mg kg^{-1}) in the southeastern and western margins, while central areas remain moderate (30.0–45.0 mg kg^{-1}). Available potassium (Kav) exhibits a scattered distribution, dominated by intermediate concentrations (200.0–300.0 mg kg^{-1}) with localized hotspots above 300 mg kg^{-1}. A detailed summary of the area distribution of these soil parameters is provided in the Supplementary Material (Supplementary Table S5).

Integrating these layers, the final SQIw map (Figure 5) delineates a clear quality zoning. In terms of surface area, the model identified that 46.22% of the irrigation scheme faces severe limitations (comprising 1.26% "Very Poor" and 44.96% "Poor"), primarily concentrated in the southern and eastern sectors. Interestingly, the area classified as "Acceptable" dominates the landscape (51.49%), acting as a broad transition zone. In contrast, "Good" quality soils are scarce (2.28%), restricted to isolated pockets scattered across the western and northeastern zones. This spatial assessment reveals a crucial insight: while 15.6% of the sampling points were "Very Poor", this extreme condition covers only 1.26% of the total interpolated area. This suggests that the most severe degradation occurs in localized hotspots, whereas the "Poor" and "Acceptable" conditions are far more extensive and continuous.

3.5 Requirements for soil management

Evaluations of the SQIw in the Bella Unión district revealed pronounced variability in organic matter (OM), available phosphorus (Pav), available potassium (Kav), recommended fertilization rates, and compost amendment requirements. Site-specific requirements were estimated according to the established SQIw categories, allowing differentiated fertilization strategies for soils classified as "Very Poor", "Poor", "Acceptable", "Good", and "Optimal". Soils classified in the degraded strata ("Very Poor" and "Poor"), characterized by critical OM levels (≤ 0.80%) and low nutrient availability, required the highest input levels. For the "Poor" category, inputs included ammonium sulfate (up to 559.27 kg ha^{-1}), monoammonium phosphate (up to 146.32 kg ha^{-1}), potassium sulfate (up to 381.75 kg ha^{-1}), and compost (up to 15.61 t ha^{-1}). As soil quality improved to "Acceptable" and "Good", the requirements for monoammonium phosphate—and particularly potassium sulfate and compost—decreased substantially, reaching 0 t ha^{-1} in the Optimal quality soils. Detailed fertilization rates and compost requirements for each SQIw class are provided in Supplementary Table S6.

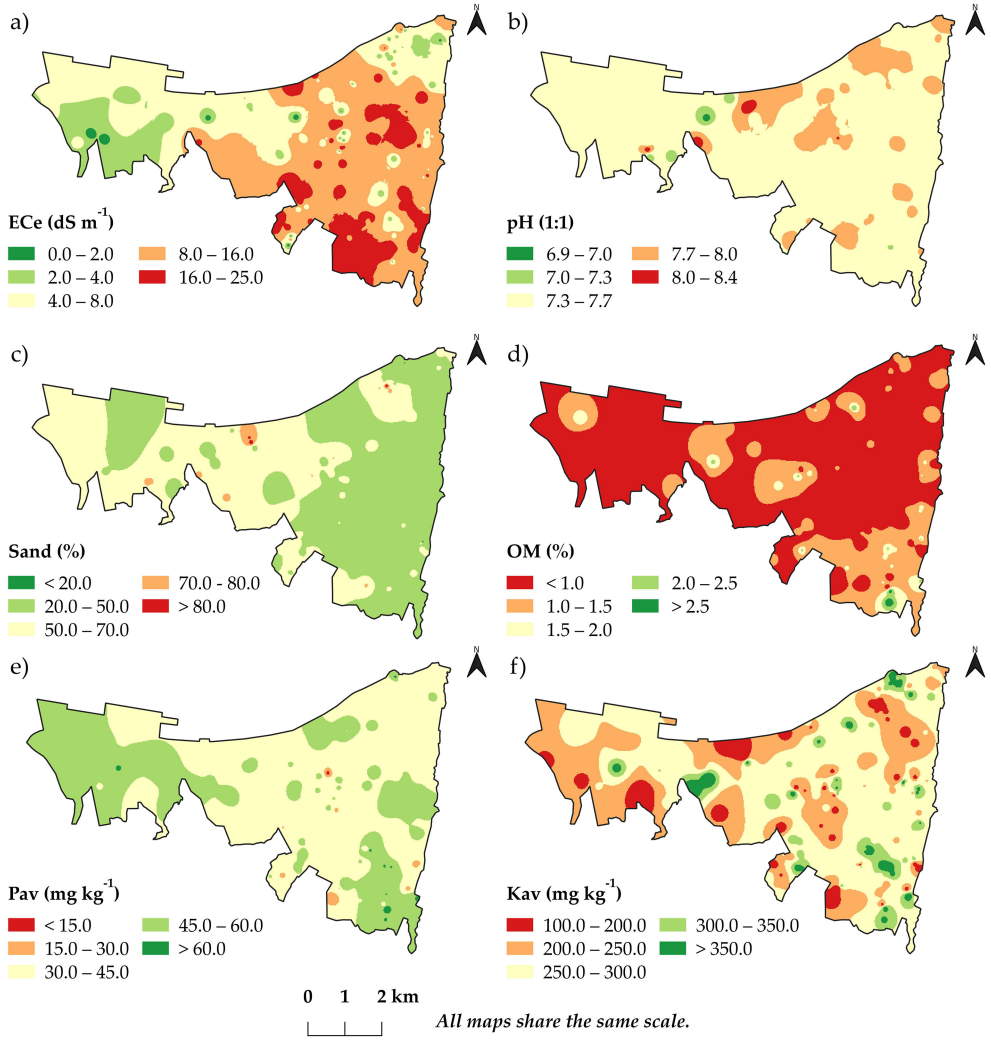

FIGURE 4
Spatial distribution of key soil indicators across the Bella Unión olive orchards. Maps were generated using IDW interpolation. **(a)** Electrical Conductivity (ECe), **(b)** pH, **(c)** Sand content, **(d)** Organic Matter (OM), **(e)** Available Phosphorus (Pav), and **(f)** Available Potassium (Kav). The color gradients represent the variability of each parameter, with specific classification thresholds detailed in the legend.

4 Discussions

4.1 Variability and main soil constraints

Soils in Bella Unión showed typical constraints of irrigated arid zones: slightly alkaline pH, low OM, and high ECe. The slightly alkaline pH (7.62 ± 0.22) is consistent with reports from calcareous soils in other arid regions, such as the Dakhla Oasis in Egypt and northeastern Iran (56, 57). This factor can reduce the availability of essential micronutrients such as Fe, Zn, and Mn (58).

Regarding salinity, the high mean ECe (10.59 ± 7.35 dS m^{-1}) represents the primary constraint, as it can reduce water uptake capacity of roots and lead to toxicity from excessive salt accumulation in plant tissues (59, 60). While values greater than 4.2 dS m^{-1} can reduce olive yield from 10–50% (8, 61), the predominant "Sevillana" variety is considered moderately tolerant which mitigate productive losses compared to sensitive cultivars (62, 63). The reliability of this diagnosis is supported by the sensitive analysis, which confirmed that the texture-based conversion uncertainty (± 2.09 dS m^{-1}) does not alter the structural classification of the valley as saline.

The high variability of ECe (CV = 69%) suggests differential salt accumulation processes, likely associated with heterogeneity of groundwater used for irrigation (64). The geostatistical analysis provided further insights, revealing that this heterogeneity is spatially structured rather than random (I = 0.196, $p < 0.05$). The predominant moderate spatial dependence suggests that salt accumulation is governed by a complex interaction between intrinsic factors and extrinsic practices, likely associated with the heterogeneity of groundwater used for irrigation. This pattern of spatial heterogeneity is characteristic of irrigated arid oases. For instance, in the Werigan–Kuqa oasis in China, ECe ranged from 0.079 to 143.4 dS m^{-1}, with a CV of 119 % (65). Similarly, pronounced spatial heterogeneity was observed in the Dakhla

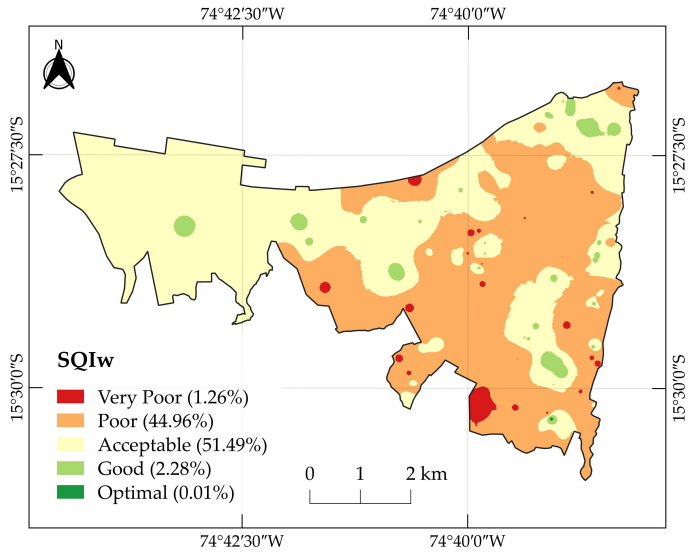

FIGURE 5
Spatial distribution map of the Soil Quality Index (SQIw) within the study area.

Oasis, Egypt, with a CV of 142.8 % and values ranging from 2.3 to 165.8 dS m^{-1} (56).

Finally, the low OM content (mean 0.95%) highlights the fragility of these arid soils, since OM supports aggregate stability, water retention, nutrient storage, and microbial activity (66, 67). The high variability observed (CV = 56%) may result from differentiated management practices and a scarcity of OM sources. The OM values (0.50–3.10%) are similar to those reported for other arid soils in southern coastal Peru (0.31–2.41% (68);).

4.2 Interactions between soil properties and fertility

The correlation matrix showed relationships that reflect fundamental edaphic processes. The negative correlation between soil ECe and clay content (ρ = −0.51) could be explained by the accumulation of salts, particularly sodium, from poor-quality groundwater irrigation (69). Such conditions promote clay dispersion and pore clogging (70), hindering effective salt leaching. From a soil fertility perspective, identifying the predominant salts is crucial, as an excess of certain ions can lead to nutritional imbalances, such as high potassium-to-calcium ratios (71). Regarding soil pH, the observed negative trend with available P (ρ = −0.24) is consistent with literature: in alkaline soils, P precipitates with cations (Ca^{2+}, Mg^{2+}) forming sparingly soluble phosphates (72, 73).

Conversely, OM enhances K availability (ρ = 0.48) by fixation and promoting solubilization for plant uptake (74, 75). However, OM content declines as sand percentage increases (ρ = −0.46) due to two factors: higher aeration accelerating decomposition, and the lack of fine particles to physically protect organic compounds (1).

Similarly, coarse textures compromise nutrient retention, accounting for the inverse link between sand and both phosphorus (ρ = −0.38) and potassium (ρ = −0.63). This texture-driven porosity facilitates significant nutrient losses via leaching or runoff (76, 77). Collectively, results confirm that while pH and salinity are significant stressors, soil texture acts as the primary regulator for organic matter and macronutrient availability in the study area.

4.3 Selection of key indicators and application of the soil quality index

The Principal Component Analysis (PCA) summarized the multivariate structure of the dataset effectively, capturing more than 76% of the total variability in only three dimensions. This reduction indicates that the selected indicators adequately represent the functional attributes of the Bella Unión soils.

Variable clustering reveals the agroecosystem's governing processes. The association of Sand, OM, and macronutrients (Pav, Kav) in the first component (PC1) statistically validates the strong dependence of fertility on soil texture, a characteristic mechanism in arid lands where coarse fractions limit organic carbon retention and nutrient cation storage. Meanwhile, the isolation of pH (PC2) and Salinity (PC3) into orthogonal components highlights them as distinct chemical stressors independent of general fertility. These findings align with research in similar arid environments, where texture regulates water-nutrient dynamics while pH and ECe act as the primary abiotic constraints in the soil profile (78).

This selection is further supported by global literature identifying OM and pH as universal indicators, followed by Pav and Kav (79). Ultimately, this approach balances statistical objectivity with practical relevance, offering a tool consistent with studies in Asian and African arid systems (80, 81).

The weighted Soil Quality Index (SQIw) highlighted severe limitations, classifying near 46% of the area as "Poor" or "Very Poor". Although 51.5% fell into the "Acceptable" category, only 2.3% achieved "Good" status, with "Optimal" areas being negligible (< 0.1%). These results indicate that despite the soil pH being within the optimal range for olive cultivation (7–8) and the high availability of P and K (41), the high overall salinity exerts an overriding constraint on soil quality.

The agronomic application of the SQIw is direct: given that nearly half of the area faces salinity-driven degradation ("Poor" category), management strategies must prioritize mitigation over mere fertilization. Since the index confirms salinity as the primary limiting factor, fertilizers with high salt index, such as potassium chloride, must be strictly avoided to prevent further soil salinization (82). Although replacing crops with salt-tolerant varieties and increasing irrigation frequency are theoretical alternatives (83), the water scarcity from May to December renders high-frequency irrigation unfeasible, reinforcing the need for precise input management to sustain the "Acceptable" areas and rehabilitate the "Poor" zones.

To contextualize the magnitude of long-term soil rehabilitation, we referenced the amount of compost needed to raise OM to the minimum target of 1% in deficient soils. Given the substantial quantities (60.56 – 319.35 t ha^{-1}), this should be viewed as a long-term guideline requiring gradual application and monitoring, rather than an immediate fix.

4.4 Practical implications: site-specific management of nitrogen, phosphorus, and potassium fertilization in saline soils of Bella Unión

In Bella Unión, 51.49% of agricultural soils are classified as "Acceptable" quality. These soils are at risk of declining to "Poor" due to high salinity, alkalinity, and low organic matter (OM) (84, 85). Low OM is critical as it provides most soil N, reinforcing the need for organic amendments such as compost, stabilized manures, and green manures (86, 87). Mineral N should be applied in split doses to reduce losses through leaching and volatilization, especially in sandy soils (84, 88).

Potassium (K) management is essential under saline conditions. Increasing the K^+/Na^+ ratio and foliar K supports osmoregulation and photosynthesis in olives (89). Although Kav in the area is moderate, fertilization is critical in sandy, low-OM zones (90).

Phosphorus (P) availability is limited by alkalinity and excess Ca^{2+}, forming insoluble compounds (90). Measured Pav does not always reflect the fraction available to plants. Foliar P of 0.1–0.3% is considered adequate; values below 0.1% limit flowering and fruit set (91, 92). Highly soluble P fertilizers (MAP or phosphoric acid) and organic amendments improve P bioavailability (86, 87, 93).

The SQIw results confirm that salinity is the dominant constraint in Bella Unión, particularly in the zones where ECe exceeds 8 dS m^{-1}. The consistently low OM values further limit nutrient retention and soil functioning. Under these conditions, management should focus on avoiding high–salt-index fertilizers and gradually incorporating low-EC organic amendments. Because these constraints vary spatially, fertilization strategies should follow the SQIw classes rather than uniform field-wide recommendations.

5 Conclusions

Soils in Bella Unión exhibit typical limitations of irrigated arid lands, particularly elevated salinity, low organic matter, and coarse textures, all of which constrain soil functional capacity. The selected indicators (sand, ECe, pH, OM, Pav, and Kav) integrated into the SQIw allowed for a clear differentiation of soil quality across the landscape, with most of the area falling within the "Poor" and "Acceptable" classes. These results establish a quantitative baseline for monitoring changes in soil quality over time.

The strong spatial variability observed in salinity and organic matter indicates that soil management should be tailored to local conditions rather than implemented uniformly. However, the present dataset provides only a partial view of the agronomic constraints. A complete assessment of soil suitability will require additional analyses, particularly of exchangeable bases, soluble ion composition, and irrigation water quality, which directly influence salinity dynamics and crop performance. In addition, the estimation of ECe from EC1:5 provides only an approximate measure of salinity status, and future work should incorporate direct saturated paste extractions to improve diagnostic accuracy in highly variable soils.

Overall, this study presents an initial characterization of soil quality in the olive-growing areas of Bella Unión and highlights priority areas for intervention, but site-specific management strategies should be refined through future work that incorporates sodicity parameters, water quality assessments, and crop response evaluations under local production conditions.

Data availability statement

The original contributions presented in the study are included in the article/Supplementary Material. Further inquiries can be directed to the corresponding author.

Author contributions

RP-C: Formal Analysis, Writing – original draft, Methodology, Conceptualization, Investigation. CV-G: Software, Formal Analysis, Writing – original draft, Methodology. SL-E: Investigation, Writing – original draft. KP-H: Methodology, Writing – original draft. AC: Investigation, Writing – original draft. MV: Writing – review & editing, Supervision. KQ: Writing – review & editing, Supervision, Writing – original draft.

Funding

The author(s) declared that financial support was received for this work and/or its publication. The work was funded by the INIA project CUI 2487112 "Mejoramiento de los servicios de investigación y transferencia tecnológica en el manejo y recuperación de suelos agrícolas degradados y aguas para riego en la pequeña y mediana agricultura en los departamentos de Lima, Áncash, San Martín, Cajamarca, Lambayeque, Junín, Ayacucho, Arequipa, Puno y Ucayali".

Conflict of interest

The author(s) declared that this work was conducted in the absence of any commercial or financial relationships that could be construed as a potential conflict of interest.

Generative AI statement

The author(s) declared that generative AI was used in the creation of this manuscript. The authors used ChatGPT (OpenAI, GPT-5.1) exclusively for grammatical editing and support in information retrieval. All generated content was critically reviewed and independently verified by the authors. Data analysis, scientific interpretation, and conclusions were performed entirely by the authors.

Any alternative text (alt text) provided alongside figures in this article has been generated by Frontiers with the support of artificial intelligence and reasonable efforts have been made to ensure accuracy, including review by the authors wherever possible. If you identify any issues, please contact us.

Publisher's note

Supplementary material

The Supplementary Material for this article can be found online at: https://www.frontiersin.org/articles/10.3389/fsoil.2026.1724235/full#supplementary-material

References

1. Weil RR, Brady NC. *The nature and properties of soils. 15th ed*. Harlow: Pearson (2017). p. 1104.

2. Smith T, Smith RL. Ambiente Terrestre. In: Ecología, *6th ed*. Pearson Educación, S.A, Madrid, España (2007). p. 87–105.

3. Daba AW. Rehabilitation of soil salinity and sodicity using diverse amendments and plants: a critical review. *Discover Environment.* (2025) 3:53. doi: 10.1007/s44274-025-00199-6

4. FAO. *Global status of salt-affected soils: Main report*. Rome, Italy: Food and Agriculture Organization of the United Nations (2024). doi: 10.4060/cd3044en

5. Maesano G, Chinnici G, Falcone G, Bellia C, Raimondo M, D'Amico M, et al. Economic and Environmental Sustainability of Olive Production: A Case Study. *Agronomy.* (2021) 11:1753. doi: 10.3390/agronomy11091753

6. Nteve GM, Kostas S, Polidoros AN, Madesis P, Nianiou-Obeidat I, Nteve GM, et al. Adaptation Mechanisms of Olive Tree under Drought Stress: The Potential of Modern Omics Approaches. *Agriculture.* (2024) 14:579. doi: 10.3390/agriculture14040579

7. El Yamani M, Cordovilla MdP. Tolerance Mechanisms of Olive Tree (Olea europaea) under Saline Conditions. *Plants.* (2024) 13:209. doi: 10.3390/plants13152094

8. Bernstein L. Salt Tolerance of Fruit Crops. In: *Agriculture Research Service*. U.S. Department of Agriculture, Washington, DC, USA (1965). p. 8.

9. Chartzoulakis KS. Salinity and olive: Growth, salt tolerance, photosynthesis and yield. *Agric Water Management.* (2005) 78:108–21. doi: 10.1016/j.agwat.2005.04.025

10. Chartzoulakis KS. The use of saline water for irrigation of olives: Effects on growth, physiology, yield and oil quality. *Acta Horticulturae.* (2011) 888):97–108. doi: 10.17660/ActaHortic.2011.888.10

11. Azimi M, Khoshzaman T, Taheri M, Dadras A. Evaluation of salinity tolerance of three olive (Olea europaea L.) cultivars. *J Cent Eur Agriculture.* (2021) 22:571–81. doi: 10.5513/JCEA01/22.3.3167

12. Katuri JR, Trifonov P, Arye G, Katuri JR, Trifonov P, Arye G. Spatial Distribution of Salinity and Sodicity in Arid Climate Following Long Term Brackish Water Drip Irrigated Olive Orchard. *Water.* (2019) 11:2556. doi: 10.3390/w11122556

13. Trabelsi L, Gargouri K, Ayadi M, Mbadra C, Ben Nasr M, Ben Mbarek H, et al. Impact of drought and salinity on olive potential yield, oil and fruit qualities (cv. Chemlali) in an arid climate. *Agric Water Management.* (2022) 269:107726. doi: 10.1016/j.agwat.2022.107726

14. Santiago-Mejía BE, Martínez-Menez MR, Rubio-Granados E, Vaquera-Huerta H, Sánchez-Escudero J, Santiago-Mejía BE, et al. Variabilidad espacial de propiedades físicas y químicas del suelo en un sistema lama-bordo en la Mixteca Alta de Oaxaca, México. *Agricultura sociedad y desarrollo.* (2018) 15:275–88.

15. U.S. Department of Agriculture, Natural Resources Conservation Service. *Guía para la evaluación de la calidad y salud del suelo*. Lincoln, Nebraska: USDA Natural Resources Conservation Service, Soil Quality Institute (1999). Available online at: https://www.nrcs.usda.gov/sites/default/files/2022-10/Guia%20para%20la%20Evaluacion%20de%20la%20Calidad%20y%20Salud%20del%20Suelo.pdf.

16. Bastida F, Zsolnay A, Hernández T, García C. Past, present and future of soil quality indices: A biological perspective. *Geoderma.* (2008) 147:159–71. doi: 10.1016/j.geoderma.2008.08.007

17. Vasu D, Singh SK, Ray SK, Duraisami VP, Tiwary P, Chandran P, et al. Soil quality index (SQI) as a tool to evaluate crop productivity in semi-arid Deccan plateau, India. *Geoderma.* (2016) 282:70–9. doi: 10.1016/j.geoderma.2016.07.010

18. Şenol H, Alaboz P, Demir S, Dengiz O. Computational intelligence applied to soil quality index using GIS and geostatistical approaches in semiarid ecosystem. *Arabian J Geosciences.* (2020) 13:1235. doi: 10.1007/s12517-020-06214-9

19. Jena RK, Moharana PC, Pradhan UK, Sharma GK, Ray P, Roy PD, et al. Soil fertility mapping and applications for site-specific nutrient management: a case study. In: *Remote Sensing of Soils*. Elsevier, Amsterdam, Netherlands (2024). 65–80. doi: 10.1016/B978-0-443-18773-5.00025-9

20. Damiba WAF, Gathenya JM, Raude JM, Home PG. Soil quality index (SQI) for evaluating the sustainability status of Kakia-Esamburmbur catchment under three different land use types in Narok County, Kenya. *Heliyon.* (2024) 10:e25611. doi: 10.1016/j.heliyon.2024.e25611

21. Hmidi O, Srarfi F, Brahim N, Dazzi C, Papa GL, Hmidi O, et al. Assessment of Soil and Water Quality Indices in Agricultural Soils of Manouba Governorate, North-East Tunisia. *Soil Systems.* (2025) 9:105. doi: 10.3390/soilsystems9030105

22. Rahmanipour F, Marzaioli R, Bahrami HA, Fereidouni Z, Bandarabadi SR. Assessment of soil quality indices in agricultural lands of Qazvin Province, Iran. *Ecol Indicators.* (2014) 40:19–26. doi: 10.1016/j.ecolind.2013.12.003

23. Colombi - Mendivil SAI, Colombi AA. *Estudio agrológico: Lote N°2 - negociación agrícola santa teresita S.A. / lote N°3 - sucesión alberto noriega duclá, irrigación pampas de la bella unión (acarí - arequipa)*. Arequipa, Perú: Autoridad Nacional del Agua (1964). Available online at: https://hdl.handle.net/20.500.12543/4269.

24. Espino Ciudad JA. *Caracterización hidrobiológica y calidad de agua en la cuenca del río Acarí (Ayacucho - Arequipa)*. Lima, Perú: Universidad Nacional Mayor de San Marcos (2017). Available online at: https://hdl.handle.net/20.500.12672/7062.

25. Instituto Nacional de Estadística e Informática (INEI). *Informe metodología y cálculo de indicadores: Resultados anuales. Encuesta Nacional Agropecuaria, 2022*. Lima, Perú: Instituto Nacional de Estadística e Informática (2023). Available online at: https://proyectos.inei.gob.pe/iinei/srienaho/Descarga/DocumentosMetodologicos/2022-62/04_INFORME_MEF_2022.pdf.

26. *Ministerio de Desarrollo Agrario y Riego del Perú (MIDAGRI). Superficie agrícola del Perú*. MIDAGRI, Lima, Peru (2024). Available online at: https://siea.midagri.gob.pe/portal/informativos/superficie-agricola-peruana.

27. *Instituto Geológico Minero y Metalúrgico (INGEMMET)*. Geocatmin: Sistema de información geológico y catastral minero (2016). Available online at: https://geocatmin.ingemmet.gob.pe/geocatmin/.

28. *Servicio Nacional de Meteorología e Hidrología del Perú (SENAMHI). Mapa climático del Perú*. (2020). Lima, Perú: SENAMHI. Available online at: https://www.senamhi.gob.pe/?&p=mapa-climatico-del-peru (Accessed September 25, 2025).

29. Castro A, Davila Arriaga C, Laura W, Cubas Saucedo F, Avalos G, López C, et al. *Climas del Perú: mapa de clasificación climática nacional. Servicio Nacional de Meteorología e Hidrología del Perú* (2021). Available online at: http://repositorio.senamhi.gob.pe/handle/20.500.12542/1336 (Accessed June 23, 2025).

30. Abate GG. Review article: Soil sampling and sample preparation. *Int J Modern Sci Res Technology*. (2025) 3:167–76. doi: 10.5281/zenodo.14810773

31. Cabrera-Rodríguez A, Nava-Reyna E, Trejo-Calzada R, Peña CGD, Arreola-Ávila JG, Collavino MM, et al. Effect of Organic and Conventional Systems Used to Grow Pecan Trees on Diversity of Soil Microbiota. *Diversity*. (2020) 12:436. doi: 10.3390/d12110436

32. Tan KH. *Soil sampling, preparation, and analysis. 2nd ed*. Boca Raton, FL: Taylor & Francis (2005).

33. Nandal A, Rani S, Yadav SS, Kaushik N, Kataria N, Hasanpuri P, et al. Soil quality under different tree species in an urban university campus: a multidimensional study. *Environ Earth Sci*. (2024) 83:613. doi: 10.1007/s12665-024-11902-w

34. International Organization for Standardization (ISO). *Soil quality — Pretreatment of samples for physico-chemical analysis (ISO 11464:2006)*. Geneva, Switzerland: International Organization for Standardization (2006). Available online at: https://www.iso.org/standard/37718.html.

35. Secretaría de Medio Ambiente y Recursos Naturales (SEMARNAT). *Norma Oficial Mexicana NOM-021-RECNAT-2000, que establece las especificaciones de fertilidad, salinidad y clasificación de suelos. Estudios, muestreo y análisis*. México, D.F: Secretaría de Medio Ambiente y Recursos Naturales (2002). Available online at: https://www.ordenjuridico.gob.mx/Documentos/Federal/wo69255.pdf.

36. United States Environmental Protection Agency (US EPA). *Method 9045D: Soil and waste pH*. Washington, DC: United States Environmental Protection Agency (2004). Available online at: https://www.epa.gov/sites/default/files/2015-12/documents/9045d.pdf.

37. International Organization for Standardization (ISO). *Soil quality — Determination of the specific electrical conductivity (ISO 11265:1994)*. Geneva, Switzerland: International Organization for Standardization (1994). Available online at: https://www.iso.org/standard/19243.html.

38. Kargas G, Londra P, Sotirakoglou K. The Effect of Soil Texture on the Conversion Factor of 1:5 Soil/Water Extract Electrical Conductivity (EC1:5) to Soil Saturated Paste Extract Electrical Conductivity (ECe). *Water*. (2022) 14:642. doi: 10.3390/w14040642

39. McBratney AB, Minasny B, Cattle SR, Vervoort RW. From pedotransfer functions to soil inference systems. *Geoderma*. (2002) 109:41–73. doi: 10.1016/S0016-7061(02)00139-8

40. Maleki S, Zeraatpisheh M, Karimi A, Sareban G, Wang L. Assessing Variation of Soil Quality in Agroecosystem in an Arid Environment Using Digital Soil Mapping. *Agronomy*. (2022) 12:578. doi: 10.3390/agronomy12030578

41. Tombesi A, Tombesi S. Orchard planning and planting. In: *Production techniques in olive growing*. International Olive Council, Madrid, Spain (2007). p. 15–40.

42. U.S. Department of Agriculture, Natural Resources Conservation Service. *Soil survey manual*. Ditzler C, Scheffe K, Monger HC, editors. Washington, DC: U.S. Government Publishing Office (2017). (USDA handbook).

43. Bati CB, Santilli E, Guagliardi I, Toscano P, Bati CB, Santilli E, et al. Cultivation Techniques. In: *Olive Germplasm - The Olive Cultivation, Table Olive and Olive Oil Industry in Italy*. IntechOpen, Rijeka, Croatia (2012). doi: 10.5772/51932

44. Saxton KE, Rawls WJ. Soil Water Characteristic Estimates by Texture and Organic Matter for Hydrologic Solutions. *Soil Sci Soc America J*. (2006) 70:1569–78. doi: 10.2136/sssaj2005.0117

45. Andrews SS, Karlen DL, Mitchell JP. A comparison of soil quality indexing methods for vegetable production systems in Northern California. *Agriculture Ecosyst Environment*. (2002) 90:25–45. doi: 10.1016/S0167-8809(01)00174-8

46. Ghimire P, Shrestha S, Acharya A, Wagle A, Acharya TD. Soil fertility mapping of a cultivated area in Resunga Municipality, Gulmi, Nepal. *PloS One*. (2024) 19: e0292181. doi: 10.1371/journal.pone.0292181

47. Moran PAP. Notes on Continuous Stochastic Phenomena. *Biometrika*. (1950) 37:17–23. doi: 10.2307/2332142

48. Cambardella CA, Moorman TB, Novak JM, Parkin TB, Karlen DL, Turco RF, et al. Field-Scale Variability of Soil Properties in Central Iowa Soils. *Soil Sci Soc America J*. (1994) 58:1501–11. doi: 10.2136/sssaj1994.03615995005800050033x

49. Robinson TP, Metternicht G. Testing the performance of spatial interpolation techniques for mapping soil properties. *Comput Electron Agriculture*. (2006) 50:97–108. doi: 10.1016/j.compag.2005.07.003

50. R Core Team. *R: A language and environment for statistical computing*. Vienna, Austria: R Foundation for Statistical Computing (2025). Available online at: https://www.R-project.org/.

51. Lê S, Josse J, Husson F. FactoMineR: An R Package for Multivariate Analysis. *J Stat Software*. (2008) 25:1–8. doi: 10.18637/jss.v025.i01

52. Pebesma EJ. Multivariable geostatistics in S: the gstat package. *Comput Geosciences*. (2004) 30:683–91. doi: 10.1016/j.cageo.2004.03.012

53. Bivand RS, Pebesma E, Gómez-Rubio V. *Applied spatial data analysis with R. 2nd ed*. New York: Springer (2013). doi: 10.1007/978-1-4614-7618-4

54. Revelle W. *psych: Procedures for psychological, psychometric, and personality research*. Evanston, Illinois: Northwestern University (2025). Available online at: https://CRAN.R-project.org/package=psych.

55. Wei T, Simko V. *R package "corrplot": Visualization of a correlation matrix* (2024). Available online at: https://github.com/taiyun/corrplot (Accessed June 26, 2025).

56. Selmy SAH, Abd Al-Aziz SH, Jiménez-Ballesta R, Jesús García-Navarro F, Fadl ME. Soil Quality Assessment Using Multivariate Approaches: A Case Study of the Dakhla Oasis Arid Lands. *Land*. (2021) 10:1074. doi: 10.3390/land10101074

57. Rezapour S, Kalashypour E. Effects of irrigation and cultivation on the chemical indices of saline–sodic soils in a calcareous environment. *Int J Environ Sci Technology*. (2019) 16:1501–14. doi: 10.1007/s13762-017-1606-6

58. Osman KT. Saline and Sodic Soils. In: Osman KT, editor. *Management of Soil Problems*. Springer International Publishing, Cham (2018). p. 255–98. doi: 10.1007/978-3-319-75527-4_10

59. Zhou H, Shi H, Yang Y, Feng X, Chen X, Xiao F, et al. Insights into plant salt stress signaling and tolerance. *J Genet Genomics*. (2024) 51:16–34. doi: 10.1016/j.jgg.2023.08.007

60. Munns R, Tester M. Mechanisms of Salinity Tolerance. *Annu Rev Plant Biol*. (2008) 59:651–81. doi: 10.1146/annurev.arplant.59.032607.092911

61. Ben-Gal A, Beiersdorf I, Yermiyahu U, Soda N, Presnov E, Zipori I, et al. Response of young bearing olive trees to irrigation-induced salinity. *Irrigation Science*. (2017) 35:99–109. doi: 10.1007/s00271-016-0525-5

62. Tabatabaei SJ. Salinity stress and olive: an overview. *Plant Stress*. (2007) 1:105–12.

63. Benlloch M, Marin L, Fernández-Escobar R. Salt tolerance of various olive varieties. In: *Acta Horticulturae*. International Society for Horticultural Science (ISHS, Leuven, Belgium (1994). p. 215–7. doi: 10.17660/ActaHortic.1994.356.46

64. Instituto Nacional de Recursos Naturales (INRENA). *Dirección General de Estudios y Proyectos. Evaluación hidrogeológica para fines de explotación de aguas subterráneas con pozos tajos abiertos - valles Acarí y Bella Unión*. Lima, Perú: Instituto Nacional de Recursos Naturales (1997). Available online at: https://hdl.handle.net/20.500.12543/3899 (Accessed September 26, 2025).

65. Ma S, He B, Xie B, Ge X, Han L. Investigation of the spatial and temporal variation of soil salinity using Google Earth Engine: a case study at Werigan–Kuqa Oasis, West China. *Sci Rep*. (2023) 13:2754. doi: 10.1038/s41598-023-27760-8

66. Lal R. Soil carbon sequestration to mitigate climate change. *Geoderma*. (2004) 123:1–22. doi: 10.1016/j.geoderma.2004.01.032

67. Lal R. Soil organic matter content and crop yield. *J Soil Water Conserv*. (2020) 75:27A–32A. doi: 10.2489/jswc.75.2.27A

68. Zúñiga L. *Transformation of the hyper-arid desert soils in Arequipa Peru during four decades of irrigated agriculture*. West Lafayette, Indiana: Purdue University (2020). Available online at: https://hammer.purdue.edu/articles/thesis/Transformation_of_the_hyper-arid_desert_soils_in_Arequipa_Peru_during_four_decades_of_irrigated_agriculture/13099850.

69. Mohanavelu A, Naganna SR, Al-Ansari N, Mohanavelu A, Naganna SR, Al-Ansari N. Irrigation Induced Salinity and Sodicity Hazards on Soil and Groundwater: An Overview of Its Causes, Impacts and Mitigation Strategies. *Agriculture*. (2021) 11:983. doi: 10.3390/agriculture11100983

70. Frenkel H, Goertzen JO, Rhoades JD. Effects of Clay Type and Content, Exchangeable Sodium Percentage, and Electrolyte Concentration on Clay Dispersion and Soil Hydraulic Conductivity. *Soil Sci Soc America J*. (1978) 42:32–9. doi: 10.2136/sssaj1978.03615995004200010008x

71. Jakobsen ST. Interaction between Plant Nutrients: III. Antagonism between Potassium, Magnesium and Calcium. *Acta Agriculturae Scandinavica Section B — Soil Plant Science*. (1993) 43:1–5. doi: 10.1080/09064719309410223

72. Havlin JL, Tisdale SL, Nelson WL, Beaton JD. Soil fertility and fertilizers: An introduction to nutrient management. *8th ed*. Noida, Uttar Pradesh, India: Pearson India Education Services Pvt. Ltd. (2014).

73. Leytem A, Mikkelsen R. The Nature of Phosphorus in Calcareous Soils. *Better Crops*. (2005) 89:11–13.

74. Olk DC, Cassman KG. Reduction of Potassium Fixation by Two Humic Acid Fractions in Vermiculitic Soils. *Soil Sci Soc America J*. (1995) 59:1250–8. doi: 10.2136/sssaj1995.03615995005900050007x

75. Bader BR, Taban SK, Fahmi AH, Abood MA, Hamdi GJ. Potassium availability in soil amended with organic matter and phosphorous fertiliser under water stress during maize (*Zea mays* L) growth. *J Saudi Soc Agric Sci*. (2021) 20:390–4. doi: 10.1016/j.jssas.2021.04.006

76. Campbell KL, Rogers JS, Hensel DR. Drainage water quality from potato production. *Trans ASAE*. (1985) 28:1798–801. doi: 10.13031/2013.32521

77. Matichenkov V, Bocharnikova E, Campbell J. Reduction in nutrient leaching from sandy soils by Si-rich materials: Laboratory, greenhouse and filed studies. *Soil Tillage Res*. (2020) 196:104450. doi: 10.1016/j.still.2019.104450

78. Andrews SS, Karlen DL, Cambardella CA. The Soil Management Assessment Framework. *Soil Sci Soc America J*. (2004) 68:1945–62. doi: 10.2136/sssaj2004.1945

79. Bünemann EK, Bongiorno G, Bai Z, Creamer RE, De Deyn G, de Goede R, et al. Soil quality – A critical review. *Soil Biol Biochem*. (2018) 120:105–25. doi: 10.1016/j.soilbio.2018.01.030

80. Barman A, Sheoran P, Yadav RK, Abhishek R, Sharma R, Prajapat K, et al. Soil spatial variability characterization: Delineating index-based management zones in salt-affected agroecosystem of India. *J Environ Management*. (2021) 296:113243. doi: 10.1016/j.jenvman.2021.113243

81. Macedo RS, Lima RP, de Almeida Alves Carneiro K, Moro L, Refati DC, Campos MCC, et al. Assessment of Soil Quality of Smallholder Agroecosystems in the Semiarid Region of Northeastern Brazil. *Land*. (2024) 13:304. doi: 10.3390/land13030304

82. Buvaneshwari S, Riotte J, Sekhar M, Sharma AK, Helliwell R, Kumar MSM, et al. Potash fertilizer promotes incipient salinization in groundwater irrigated semi-arid agriculture. *Sci Rep*. (2020) 10:3691. doi: 10.1038/s41598-020-60365-z

83. Melgar JC, Mohamed Y, Serrano N, García-Galavís PA, Navarro C, Parra MA, et al. Long term responses of olive trees to salinity. *Agric Water Management*. (2009) 96:1105–13. doi: 10.1016/j.agwat.2009.02.009

84. Giller KE, Cadisch G, Ehaliotis C, Adams E, Sakala WD, Mafongoya PL. Building Soil Nitrogen Capital in Africa. In: *Replenishing Soil Fertility in Africa*. John Wiley & Sons, Ltd, Wisconsin, USA (1997). 151–92. doi: 10.2136/sssaspecpub51.c7

85. Lal R. Soil Carbon Sequestration Impacts on Global Climate Change and Food Security. *Science*. (2004) 304:1623–7. doi: 10.1126/science.1097396

86. Mahdi HH, Mouhamad RS. Behavior of phosphorus in the calcareous soil. *Adv Agric Technol Plant Sci*. (2018) 1:180018.

87. Khan KS, Ali MM, Naveed M, Rehmani MIA, Shafique MW, Ali HM, et al. Co-application of organic amendments and inorganic P increase maize growth and soil carbon, phosphorus availability in calcareous soil. *Front Environ Science*. (2022) 10:949371. doi: 10.3389/fenvs.2022.949371

88. Hu C, Sadras VO, Lu G, Zhang P, Han Y, Liu L, et al. A global meta-analysis of split nitrogen application for improved wheat yield and grain protein content. *Soil Tillage Res*. (2021) 213:105111. doi: 10.1016/j.still.2021.105111

89. Boussadia O, Zgallai H, Mzid N, Zaabar R, Braham M, Doupis G, et al. Physiological Responses of Two Olive Cultivars to Salt Stress. *Plants*. (2023) 12:1926. doi: 10.3390/plants12101926

90. Haberman A, Dag A, Shtern N, Zipori I, Erel R, Ben-Gal A, et al. Long-Term Impact of Potassium Fertilization on Soil and Productivity in Intensive Olive Cultivation. *Agronomy*. (2019) 9:525. doi: 10.3390/agronomy9090525

91. Centeno A, Gómez del Campo M. Response of mature olive trees with adequate leaf nutrient status to additional nitrogen, phosphorus, and potassium fertilization. *Acta Horticulturae*. (2011) 888:277–80. doi: 10.17660/ActaHortic.2011.888.31

92. Haberman A, Dag A, Erel R, Zipori I, Shtern N, Ben-Gal A, et al. Long-Term Impact of Phosphorous Fertilization on Yield and Alternate Bearing in Intensive Irrigated Olive Cultivation. *Plants*. (2021) 10:1821. doi: 10.3390/plants10091821

93. Brownrigg S, McLaughlin MJ, McBeath T, Vadakattu G. Effect of acidifying amendments on P availability in calcareous soils. *Nutrient Cycling Agroecosystems*. (2022) 124:247–62. doi: 10.1007/s10705-022-10241-1